

## Electron-beam-induced "explosive" crystallization of amorphous $\text{Se}_{80}\text{Te}_{20}$ alloy thin films and oriented growth of crystallites

V. Damodara Das and P. Jansi Lakshmi

*Thin Film Laboratory, Department of Physics, Indian Institute of Technology, Madras 600 036, India*

(Received 12 January 1987; revised manuscript received 10 August 1987)

Thin films of  $\text{Se}_{80}\text{Te}_{20}$  were prepared by vacuum evaporation of the polycrystalline bulk alloy at a fast rate onto replicating tape pieces held at room temperature in a vacuum of  $5 \times 10^{-5}$  Torr. The alloy films were separated from the tape by dissolving the latter in acetone and were examined in an electron microscope at low electron-beam currents ( $8 \mu\text{A}$ ). The films were found to be amorphous. On increasing the electron-beam current (to a maximum of  $60 \mu\text{A}$ ), the films were found to crystallize very quickly into either polycrystalline or more than one single-crystalline orientation, as observed by the disappearance of the diffuse rings and the appearance of systematic spot patterns and sharp ring patterns. The analysis of the spot patterns revealed that more than one orientation usually occurred in single-crystalline regions. Thus, it is found that  $\text{Se}_{80}\text{Te}_{20}$  amorphous thin films crystallize in the electron microscope due to electron-beam interaction and lead to more than one single-crystalline orientation of the phase-transformed films. The very fast rate of crystallization, the crystallization of the entire film by irradiation of only one spot, and the observed dendritic growth features confirm that the electron-beam-induced crystallization is "explosive."

### INTRODUCTION

Two of the exhaustive earlier works on electron-beam effects on thin films of various materials were made by Dart<sup>1</sup> and Levenstein.<sup>2</sup> Levenstein<sup>2</sup> studied the effect of electron beams on various metals and found that low melting and boiling point materials are affected to a larger extent. Spyridelis *et al.*<sup>3</sup> showed that the temperature rise in the electron-microscope specimens under the influence of electron beams may even be of the order of  $1000^\circ\text{C}$  under suitable conditions. They have also stated that the rise in temperature would be particularly high in specimens with low thermal conductivity where heat is very slowly dissipated. Dart<sup>1</sup> even found that a prolonged exposure to the intense electron beam caused the evaporation of the material of the film. Since then, several workers have reported amorphous-crystalline transition and agglomeration effects in thin films under the action of the beam (Evans,<sup>4</sup> Srivastava,<sup>5</sup> Patel and Damodara Das<sup>6</sup>). Evans<sup>4</sup> found that the initially amorphous sputtered CdS films crystallize due to electron bombardment. Srivastava<sup>5</sup> reported crystallization and grain growth resulting from electron-beam heating of local small areas inside an electron microscope in thin polycrystalline materials of lead and palladium. Since the observations of Takamori *et al.*<sup>7,8</sup> and Messier *et al.*<sup>9</sup> during the early 1970s, where a very accelerated crystallization, termed "explosive" crystallization, had taken place even at room temperature in thick amorphous thin films of germanium using various techniques like mechanical pricking of the film and a momentary laser-beam pulse heating, a number of studies have been carried out by many workers using not only laser pulse heating but also by electron-beam heating on other amorphous materials, to investigate the phenomenon of "explosive" crystallization.

An amorphous-crystalline transition in Se and Te thin

films by a number of methods has been studied by various workers. Kim and Turnbull studied the crystallization of Se films by heating<sup>10</sup> and by light.<sup>11</sup> Chiang and Johnson<sup>12</sup> studied the effect of chemical contamination on crystallization. Hamert and Saucier<sup>13</sup> studied the influence of mechanical strain on crystallization, while Bolotov and Kamarova<sup>14</sup> studied the influence of electric field on the crystallization of Se and Te thin films. The effect of substrates on crystallization was studied by Okuyama *et al.*<sup>15</sup>

The aging effect was studied by Audiese *et al.*,<sup>16</sup> while electron- and ion-bombardment-induced crystallization has been studied by Vance.<sup>17</sup>

Amorphous-crystalline phase transformation and grain growth in thin Te-Se alloy films have been studied at different temperatures as a function of time by Vermaak and Petruzzello<sup>18</sup> while Garg *et al.*<sup>19</sup> have studied the crystallization and electrical properties of Te-Se alloy thin films. They have reported how the electrical conductivity and activation energy are affected by the presence of 0–100 at. % tellurium in the films. Otenda *et al.*<sup>20</sup> have investigated the photocrystallization of amorphous Se-Te films and distinguish between the effects induced by light illumination and thermal heating. They have also reported the growth velocity of nucleation for crystallization taking place at the interface between the film and the substrate. However, to the best of our knowledge, no previous study has been reported on the electron-bombardment-induced amorphous-crystalline transition in Se-Te alloy thin films.

We have been interested in the Se-Te alloy system to investigate whether it is possible to use these alloys in the thin-film state as memory-switching devices. As part of this study, we have been investigating the  $\text{Se}_{80}\text{Te}_{20}$  alloy films and amorphous-crystalline transition in them. In our earlier papers, we have reported amorphous-crystalline transition during heating in  $\text{Se}_{80}\text{Te}_{20}$  (Ref. 21)

and  $\text{Se}_{50}\text{Te}_{50}$  (Ref. 22) thin films. In our present study, we report how the initially amorphous  $\text{Se}_{80}\text{Te}_{20}$  alloy thin films crystallize fully at a fast rate (explosive crystallization) during examination in the electron microscope because of the electron-beam irradiation. We also show that different parts of the film are polycrystalline and also single crystalline with different orientations.

### EXPERIMENTAL

$\text{Se}_{80}\text{Te}_{20}$  bulk alloy was prepared by heating a stoichiometric mixture (4:1) of the components selenium and tellurium of purity 99.999% in a vacuum-sealed quartz tube at a temperature of 220°C for three days and at 450°C for one day, followed by slow cooling to room temperature. While heating the sample, the tube was frequently shaken to homogenize the resulting alloy. The x-ray powder photography of the samples from a number of regions of the ingot revealed that the alloy was polycrystalline and homogeneous. The unit-cell dimensions were found to be  $c = 5.137 \text{ \AA}$  and  $a = 4.392 \text{ \AA}$ , which are in agreement with earlier reported values.<sup>23</sup>

$\text{Se}_{80}\text{Te}_{20}$  films of about 700 Å thickness were prepared by deposition of the bulk  $\text{Se}_{80}\text{Te}_{20}$  alloy at a rapid rate onto replicating tape pieces held at room temperature in a standard vacuum deposition system at a pressure of  $5 \times 10^{-5}$  Torr. As there is every possibility of one of the components (Se) of the alloy preferentially evaporating during vacuum deposition of the alloy, the composition of the bulk alloy left over in the boat after an evaporation can be different from the starting bulk alloy. As a consequence, the films prepared using the leftover alloy will have a different composition. In addition, during a single evaporation the composition of the bulk alloy can change with time. Therefore, to minimize fractionation of the alloy during evaporation and to maintain the average composition of the films formed as that of the starting bulk alloy, in a given vacuum deposition, a known quantity of the bulk alloy was taken in the Mo boat as the charge, and it was completely evaporated at a fast rate to prepare the films in the present study. The alloy films deposited on replicating tape pieces were separated from the tape by allowing the latter to dissolve in acetone. The films of  $\text{Se}_{80}\text{Te}_{20}$  floating freely on acetone were lifted onto copper grids and were dried before observation in the electron microscope. The films were examined and electron bombarded with a 100-KeV electron beam in the electron microscope. The films were examined both under low and high beam currents. The aperture diameter was 200 μm.

### RESULTS

Figure 1(a) is an electron micrograph of the  $\text{Se}_{80}\text{Te}_{20}$  film before electron bombardment at very low beam currents (8 μA). The electron diffraction pattern [Fig. 1(b)] of the same region as that of Fig. 1(a) shows the amorphous nature of the  $\text{Se}_{80}\text{Te}_{20}$  film as the diffraction pattern is totally diffuse. Calculations made from the photometric recordings of the diffuse rings of this amorphous film pattern indicate that the average lattice spacings ( $d$  values) are 3.816 and 2.181 Å, and there is a

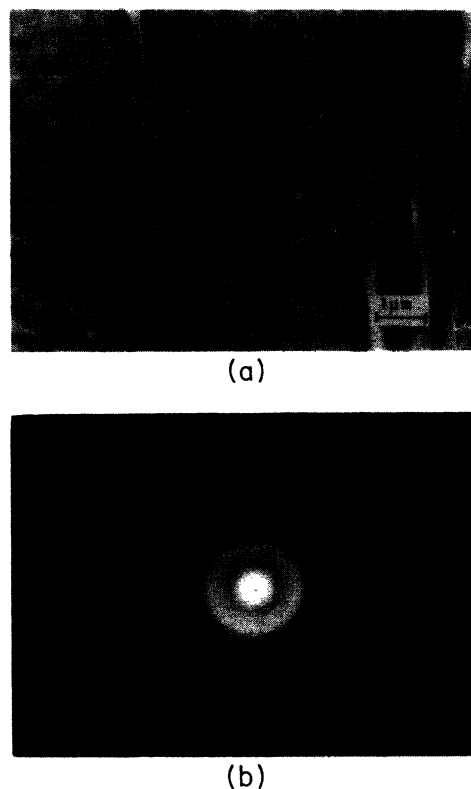
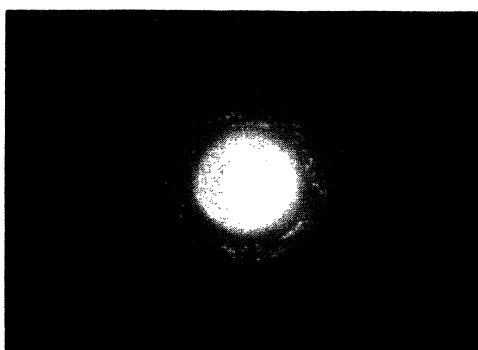


FIG. 1. (a) Electron micrograph of initial  $\text{Se}_{80}\text{Te}_{20}$  film ( $\times 10000$ ). (b) Selected area diffraction pattern of the region in (a) showing amorphous nature of the initial film.

large spread in the spacings of 23% and 10%, respectively. Figure 2(a) shows the same region after a short time (< 30 s) of bombardment at 16 μA. The appearance of dark and bright lines in the micrograph indicates that the crystallization has taken place. The corresponding diffraction pattern in Fig. 2(b) which shows sharp, spotty discontinuous rings in addition to diffuse rings reveals the inhomogeneous, transition stage; the film consisting of a mixture of both amorphous and polycrystalline phases. Figure 3(a) shows the electron micrograph after further bombardment (< 60 s) at the same current and shows full crystallization. Crystalline masses of different sizes are clearly seen in the micrograph. Figure 3(b) shows the selected area diffraction pattern corresponding to Fig. 3(a). The grainy ring pattern suggests that the crystallites of the film are sufficiently large in comparison to the beam aperture to give rise to graininess in the rings of the diffraction pattern. Also, there is no preferred orientation of the crystallites, even though the nonuniform intensity of the rings along the circumference indicates a preferential tendency. Table I shows a comparison of calculated  $d$  values (lattice spacings) from the grainy ring pattern of Fig. 3(b) with the "standard"  $d$  values of  $\text{Se}_{80}\text{Te}_{20}$  calculated from the data of Grison.<sup>23</sup> It is seen that there is a good agreement and hence the film material is  $\text{Se}_{80}\text{Te}_{20}$ . It may also be pointed out here that the average lattice spacings ( $d$  values) evaluated from the amorphous film pattern of

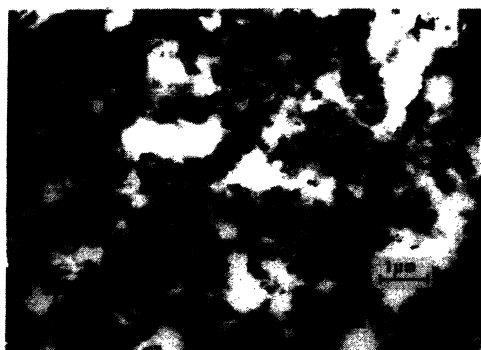


(a)



(b)

FIG. 2. (a) Same region as of Fig. 1(a) after some electron bombardment ( $\times 20000$ ). (b) Selected area diffraction pattern of the region in (a).



(a)



(b)

FIG. 3. (a) Same region as of Figs. 1(a) and 2(a) after further bombardment ( $\times 10000$ ). (b) Selected area diffraction pattern of the region in (a).

TABLE I. Comparison of calculated  $d$  values from the ring pattern of Fig. 3(b) with the standard  $d$  values of  $\text{Se}_{80}\text{Te}_{20}$ .

Serial No.	$d_{\text{calc}}$ Å	$d_{\text{standard}}$ (Å) ( $\text{Se}_{80}\text{Te}_{20}$ )	( $hkl$ )
1	5.14	5.136	(001)
2	3.84	3.804	(100)
3	3.09	3.057	(101)
4	2.18	2.196	(110)
5	1.99	2.019	(111)
6	1.89	1.902	(200)
7	1.66	1.669	(112)
8	1.36	1.384	(121)

Fig. 1(b), viz., 3.816 and 2.181 Å, correspond very well with the standard  $d$  values of the crystalline phase, viz., 3.804 and 2.196 Å, indicating also that the amorphous phase nearest-neighbor distances correspond to those of the crystalline phase. The agreement of  $d$  values of the amorphous and crystalline phases also shows that the amorphous and crystalline materials have the same composition, and hence there is no alloy disintegration.

On increasing the electron-beam current further (to a maximum of 60  $\mu\text{A}$ ), almost instantaneously the microstructure of the film changes as shown in the electron micrograph of Fig. 4(a). The diffraction pattern [Fig. 4(b)] shows a sharp ring pattern, indicating that the material is polycrystalline. The calculations made on the above pattern in Fig. 4(b) also show that the diffraction rings are due to polycrystalline  $\text{Se}_{80}\text{Te}_{20}$  and the alloy has not decomposed until now. A prolonged exposure to the intense electron beam caused the evaporation of the material to some extent. A similar observation has also been made by Levenstein<sup>2</sup> and Dart<sup>1</sup> on other materials.

In some cases, the interaction of the high-current-density electron beam with the amorphous film specimen leads to crystallization into a single-crystalline phase (with more than one single-crystalline orientation). That is, in some regions of the crystallized film, the grains are large enough compared to the aperture diameter so that single-crystalline diffraction patterns are obtained. Figures 5(a) and 5(b) show the result of electron bombardment of another initially amorphous thin-film specimen. The selected area diffraction pattern in Fig. 5(b) shows a systematic arrangement of diffraction spots which are quite sharp, indicating that the aggregates are single crystalline with apparently hexagonal morphology as seen from the electron micrograph in Fig. 5(a). Analysis of the spot pattern in Fig. 5(b) as described below reveals that more than one orientation occurs in single-crystalline regions. That is to say, in a single region even the neighboring large single-crystalline grains have different orientations.

Figures 5(c) and 5(d) show the (010) and (001) reciprocal-lattice sections of  $\text{Se}_{80}\text{Te}_{20}$  prepared by using the standard  $d$  values of  $\text{Se}_{80}\text{Te}_{20}$ , to the same scale as the the diffraction pattern in Fig. 5(b). Table II gives the comparison of the  $d$  values from the spot pattern of Fig. 5(b) with the standard  $d$  values for the reciprocal-lattice sections shown in Figs. 5(c) and 5(d). From Table II we see that the  $d$  values match well with those of  $\text{Se}_{80}\text{Te}_{20}$ .

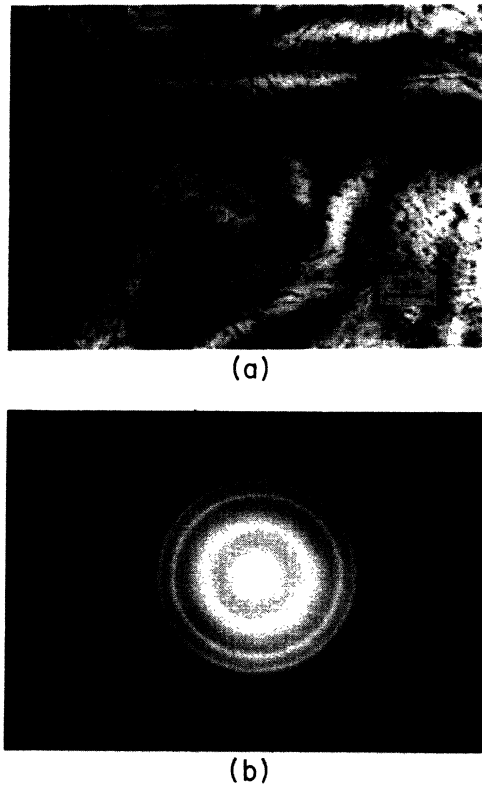


FIG. 4. (a) Electron micrograph showing the effect of increased beam intensity ( $\times 10\,000$ ). (b) Selected area diffraction pattern of the region in (a).

Figure 5(e) shows the composite reciprocal-lattice points network (CRLP network) formed by superposing the two lattice sections in Figs. 5(c) and 5(d). A comparison of the diffraction pattern in Fig. 5(b) with the CRLP network of Fig. 5(e) shows that most of the spots are accounted for. Thus, it can be concluded that the spot pattern of Fig. 5(b) arises due to more than one single-crystalline crystallite oriented such that their zone axes

TABLE II. Comparison of the  $d$  values of the spot pattern of Fig. 5(b) with the standard  $d$  values of  $\text{Se}_{80}\text{Te}_{20}$ .

Serial No.	$d_{\text{calc}}$ (Å)	$d_{\text{standard}}$ (Å) ( $\text{Se}_{80}\text{Te}_{20}$ )	( $hkl$ )
1	3.81	3.804	(100)
2	2.08	2.128	(102)
3	2.44	2.568	(002)
4	1.25	1.284	(004)
5	1.20	1.216	(104)
6	1.52	1.528	(202)
7	1.83	1.902	(200)
1	3.81	3.804	(100)
2	2.43	2.196	(110)
3	1.83	1.902	(200)
4	1.48	1.437	(210)

[010] and [001] are parallel to the electron beam. The observation that the crystallites have their [010] and [001] zone axes parallel to the electron beam (perpendicular to the film plane) is in accordance with the observation of Vermaak and Petruzzello.<sup>18</sup> It should also be pointed out that there exist two more networks of spots, both corresponding to the (010) reciprocal-lattice section of  $\text{Se}_{80}\text{Te}_{20}$ , but with their origins located on the 100 or  $0\bar{1}0$  and  $\bar{1}00$  or 010 reciprocal-lattice points of the (001) reciprocal-lattice section as shown in Fig. 5(f). These networks would arise due to double-diffraction effects. Figure 5(g) shows the superposition of the reciprocal-lattice points in Figs. 5(e) and 5(f). A comparison of this figure with the electron diffraction pattern in Fig. 5(b) shows that almost all the spots in the latter are accounted for. Thus, it can be concluded from the above that in some cases (when the electron beam is intense) initially amorphous  $\text{Se}_{80}\text{Te}_{20}$  alloy thin films crystallize into a single-crystalline phase (with more than one orientation).

It is possible that during the electron bombardment, the composition of the alloy gets altered to some extent, as can be inferred by the deviations of the calculated  $d$  values of rings and spots from the standard  $d$  values of  $\text{Se}_{80}\text{Te}_{20}$ . However, it appears to be very unlikely that pure Se (or Te) segregates during the electron bombardment, because of the absence of rings or spots corresponding to the pure elements in the diffraction patterns.

## DISCUSSION

The observation has been made that electron-beam irradiation with a beam current of  $16\ \mu\text{A}$  during observation in the electron microscope causes changes in the  $\text{Se}_{80}\text{Te}_{20}$  alloy films, which though fast are not instantaneous as during irradiation with high electron-beam currents above  $16\ \mu\text{A}$  (up to  $60\ \mu\text{A}$ ). This observation clearly indicates that there is a critical current density of the beam above which instantaneous (explosive) crystallization of the films takes place. Also, particularly during higher currents of the electron beam, the observation that the entire film on the grid (2 mm diameter) gets crystallized (either polycrystalline or single crystalline) clearly indicates that this crystallization is a very fast process unlike in the case of thermal heating. However, the major effect of the beam during amorphous-crystalline transition is apparently the heating effect raising the temperature of the alloy film above the crystallization temperature.

We have reported in our earlier papers<sup>21,22</sup> that  $\text{Se}_{80}\text{Te}_{20}$  and  $\text{Se}_{50}\text{Te}_{50}$  films which are amorphous when vacuum deposited at room temperature, undergo an amorphous-crystalline transition between 320 and 360 K upon heating in vacuum, and also exhibit a sharp discontinuity in their electrical conductivity during the transition. As the temperature of transition 320–360 K is only about 20–60 °C above room temperature, it is reasonable to state that it can be reached by the electron bombardment even at low beam currents (of the order of  $16\ \mu\text{A}$ ). As a matter of fact, similar observations on cry-

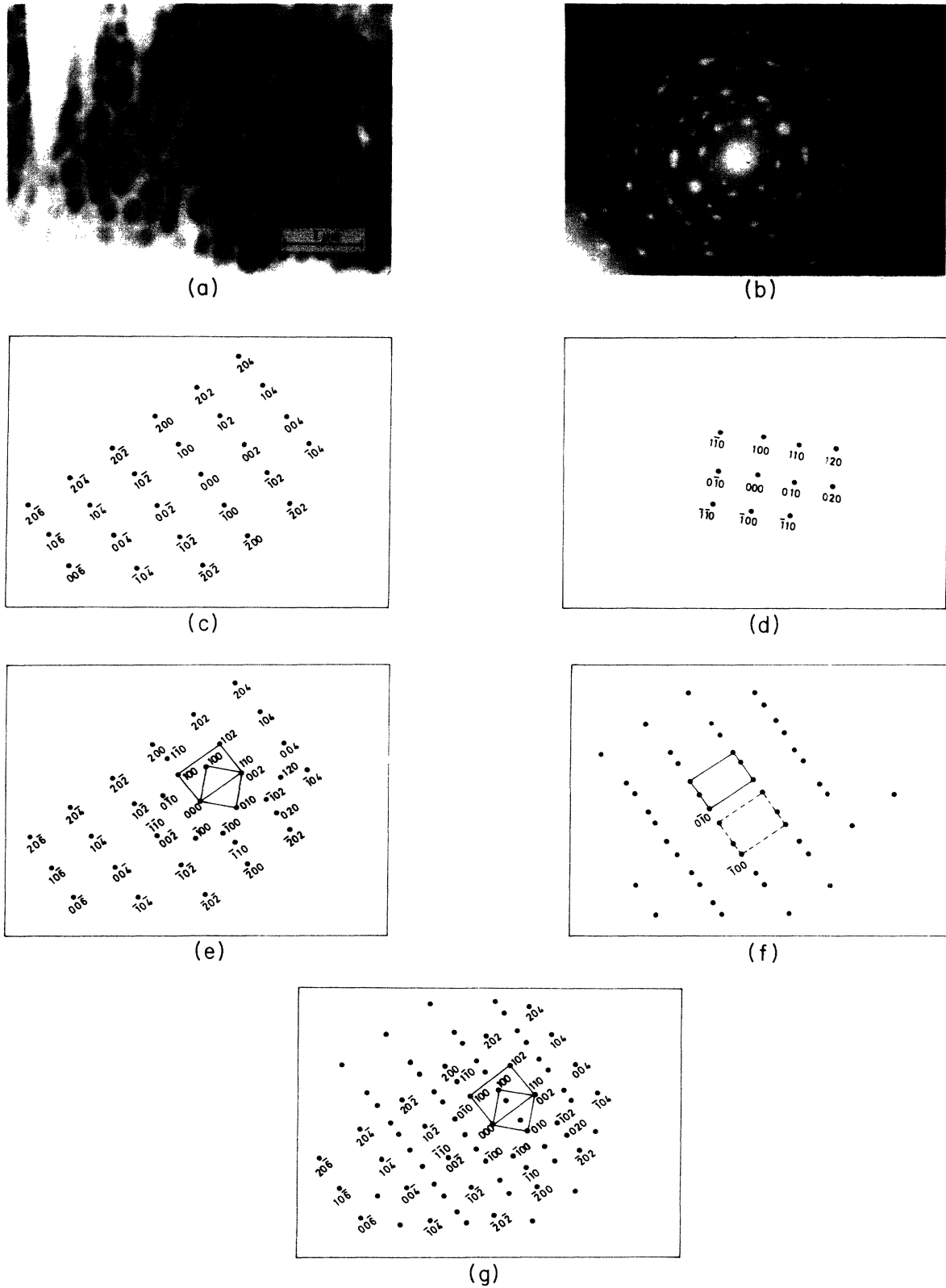


FIG. 5. (a) Electron micrograph of another amorphous specimen after bombardment showing single-crystalline aggregates with apparently hexagonal morphology ( $\times 20000$ ). (b) Selected area diffraction pattern of the region in (a). (c) (010) reciprocal-lattice section of  $\text{Se}_{80}\text{Te}_{20}$ . (d) (001) reciprocal-lattice section of  $\text{Se}_{80}\text{Te}_{20}$ . (e) Composite reciprocal-lattice point network (CRLP network) formed by superposing the two lattice sections in (c) and (d). (f) Reciprocal-lattice point networks corresponding to (010) reciprocal-lattice section with origins at  $0\bar{1}0$  and  $\bar{1}00$  reciprocal-lattice points of (001) reciprocal-lattice section. (g) CRLP network formed by superposing the reciprocal-lattice point networks of (e) and (f).

stallization of Se-Te films even below room temperature and at low beam currents were performed by Vermaak and Petruzzello.<sup>18</sup> Because of the electron-beam irradiation during observation in the electron microscope, Vermaak and Petruzzello<sup>18</sup> had to work with the lowest possible beam currents during their studies on the effects of aging on crystallization of Se-Te films at different temperatures below that of room temperature. Because of this fast crystallization of the amorphous films during electron-beam irradiation at room temperature, the kinetic studies involving time measurement could not be carried out. As a matter of fact, Vermaak and Petruzzello<sup>18</sup> have found that the growth rates of Te-Se single crystals in amorphous thin films at room temperature (about 300 K) are as much as 100 times larger than those at 273 K in the absence of the beam.

As the major effect of the electron beam is the heating effect, the observation that below about 16  $\mu\text{A}$  beam current no crystallization takes place implies that the temperature has not reached the critical temperature for crystallization under the present level of electron-beam current density. Thus, the existence of a critical temperature for crystallization leads to the existence of a critical electron-beam current density only above which the crystallization is possible. Further, this critical current density is very low because the critical temperature would be below about 320 K, the lower limit of transition temperature during the thermal crystallization of Se-Te films.<sup>21,22</sup>

Crystallization of the amorphous film under the action of the beam would also proceed in the same way as during thermal heating, viz., by formation of crystalline nuclei in the amorphous matrix, which grow, coalesce, and reorient to give rise to either polycrystalline or single-crystalline phases. However, compared to thermally induced crystallization, the electron-beam-induced crystallization is very fast so that it can be termed "explosive" crystallization. Explosive crystallization has been observed by many workers on different materials both by electron-beam irradiation<sup>24-29</sup> and by pulsed-laser annealing.<sup>8,30,31</sup> Explosive crystallization is a self-sustaining crystallization of amorphous thin films; the reason is that first the spot of the film on which the beam falls is heated to a temperature above the crystallization temperature of the amorphous film (which would even melt the film spot). This melted region would resolidify, leading to crystallization with the liberation of latent heat of fusion. This added energy would heat the neighboring region also and raise its temperature above the critical temperature, thereby melting this region also. The process could go on until the heat liberated is not sufficient enough to heat the region of the film sufficiently away from the beam above the critical temperature. In that case, a circular region of a given diameter with the center at the beam spot will be crystallized and the region outside this circular region will remain amorphous. Further, the process of crystallization will be very fast, and pulse duration of the electron beam of the order of tens of ns would be sufficient to crystallize a large circular region. Also, the growth will be generally dendritic as the rate of crystallization is very high. For

example, Fitzgerald<sup>27</sup> and Sharma *et al.*<sup>32</sup> observed crystallization of the very large circular regions of amorphous films of Ge by electron-beam irradiation. The crystallized regions were greater than 100  $\mu\text{m}$  diameter, in the former case, and 120  $\mu\text{m}$  (in diameter) in the latter case, and were nearly circular in shape. Also, the largest grain diameters observed in the former case were of the order of 20  $\mu\text{m}$  and single-crystalline electron diffraction patterns (spot patterns) were obtained. Similar crystallization of large areas of the amorphous film has also been observed during pulsed laser annealing.

In the case of our  $\text{Se}_{80}\text{Te}_{20}$  alloy films, because the crystallization temperature is only slightly above the room temperature, this temperature can be reached even with moderate electron-beam currents throughout the entire region of the film due to beam irradiation only at one spot. Thus, our observation of crystallization of the entire film (2 mm diameter) is due to the lower crystallization temperature of the alloy and hence a lower critical electron-beam current density.

It is interesting to observe that in one of the micrographs [Fig. 2(a)] where the crystallization takes place only partially [Fig. 2(b)] periodic structures (bright lines of spacings 2000  $\text{\AA}$  interspersed by dark regions) are seen. These periodic surface features are due to differential heating of the surface. Similar observations have also been made by Oron and Sorensen<sup>33</sup> on laser-annealed Si. Similar periodic structures have also been observed by Leamy *et al.*<sup>34</sup> and Maracas *et al.*<sup>35</sup> The dendritic growth features shown in Fig. 4(a), indicating very fast growth rates to form polycrystalline crystallization [cf. Fig. 4(b)], are quite common features in explosively crystallized films. For example, similar dendritic growth features have been observed in electron-beam-induced explosively crystallized amorphous thin films of Ge by Takamori *et al.*,<sup>7</sup> Fitzgerald,<sup>27</sup> and Sharma *et al.*<sup>32</sup> The electron-beam-induced (dendritic) growth and crystallization have also been observed in GeTe films by Bostanjoglo<sup>28</sup> and in Sb films by Bostanjoglo and Schlotzhauer.<sup>26</sup>

## CONCLUSIONS

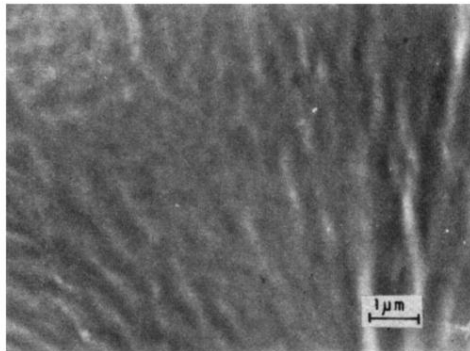
Initially amorphous  $\text{Se}_{80}\text{Te}_{20}$  alloy thin films are found to crystallize into polycrystalline or single-crystalline phase due to electron-beam interaction in the electron microscope. It is found that more than one single-crystalline orientation occurs in the single-crystalline region (e.g., [001] and [010] zone-axis orientations). Further, when exposed to the intense electron beam for longer durations, the films melt and evaporate as is expected of low melting and boiling point materials. The crystallization arising due to controlled bombardment clearly suggests that the nucleation of crystalline phase and grain growth, which occur on heat treatment, occur during electron bombardment also but at much faster rates. These observations indicate that the major effect of the electron beam is the heating effect, and hence there exists a similarity in the nature of changes brought about by heat treatment and electron-beam interaction, again with a difference that the rate of crystallization is very high. The very high rate of crystallization can be

termed "explosive" crystallization. The very small time of crystallization, large regions of the film being crystallized, the dendritic growth features observed confirm the conclusion that the crystallization taking place is "explosive."

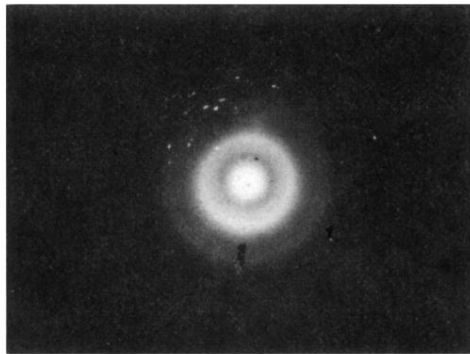
#### ACKNOWLEDGMENTS

The authors are thankful to Mrs. D. Kanchanamala of the Electron Microscopy Laboratory for the experimental assistance.

- 
- <sup>1</sup>F. E. Dart, *Phys. Rev.* **78**, 761 (1950).  
<sup>2</sup>K. Levenstein, *J. Appl. Phys.* **20**, 306 (1949).  
<sup>3</sup>J. Spyridelis, P. Delavignette, and S. Amelineckx, *Phys. Status Solidi* **19**, 683 (1967).  
<sup>4</sup>J. C. Evans, *J. Cryst. Growth* **2**, 184 (1968).  
<sup>5</sup>O. N. Srivastava, *Thin Solid Films* **3**, 127 (1969).  
<sup>6</sup>A. R. Patel and V. Damodara Das, *Thin Films* **2**, 7 (1971).  
<sup>7</sup>T. Takamori, R. Messier, and R. Roy, *Appl. Phys. Lett.* **20**, 201 (1972).  
<sup>8</sup>T. Takamori, R. Messier, and R. Roy, *J. Mater. Sci.* **8**, 1809 (1973).  
<sup>9</sup>R. Messier, T. Takamori, and R. Roy, *Solid State Commun.* **16**, 311 (1975).  
<sup>10</sup>K. S. Kim and D. Turnbull, *J. Appl. Phys.* **44**, 5237 (1973).  
<sup>11</sup>K. S. Kim and D. Turnbull, *J. Appl. Phys.* **45**, 344 (1973).  
<sup>12</sup>Y. S. Chiang and J. K. Johnson, *J. Appl. Phys.* **38**, 1647 (1967).  
<sup>13</sup>H. M. Hamert and H. Saucier, *C. R. Acad. Sci. Ser. B* **270**, 1492 (1970).  
<sup>14</sup>I. E. Bolotov and L. I. Kamarova, *Issled. Sferoloinoi Krist.* **52**, 143 (1972).  
<sup>15</sup>K. Okuyama, M. Chiba, and Y. Kumayai, *Jpn. J. Appl. Phys.* **18**, 507 (1979).  
<sup>16</sup>J. P. Audiere, Ch. Mazreres, and J. C. Carbolles, *J. Non-Cryst. Solids* **34**, 37 (1979).  
<sup>17</sup>D. W. Vance, *J. Appl. Phys.* **42**, 5430 (1971).  
<sup>18</sup>J. S. Vermaak and J. Petruzzello, *J. Appl. Phys.* **53**, 6809 (1982).  
<sup>19</sup>J. C. Garg, S. K. Jain, and B. C. Jain, *Indian J. Pure Appl. Phys.* **19**, 319 (1981).  
<sup>20</sup>M. Okuda, T. Matsushita, and A. Suzuki, *Physics of Selenium and Tellurium* (Konigstein, Germany, 1979), p. 270.  
<sup>21</sup>V. Damodara Das and P. Jansi Lakshmi, *J. Mater. Sci.* **22**, 2377 (1987).  
<sup>22</sup>V. Damodara Das and P. Jansi Lakshmi, *J. Appl. Phys.* **62**, 2376 (1987).  
<sup>23</sup>E. Grison, *J. Chem. Phys.* **19**, 1109 (1951).  
<sup>24</sup>P. Baeri, G. Foti, J. M. Poate, and A. G. Cullis, *Phys. Rev. Lett.* **45**, 2036 (1980).  
<sup>25</sup>K. Shimizu, G. E. Thompson, and G. C. Wood, *Thin Solid Films* **77**, 313 (1981).  
<sup>26</sup>O. Bostanjoglo and G. Schlotzhauer, *Phys. Status Solidi A* **68**, 555 (1981).  
<sup>27</sup>A. G. Fitzgerald, *J. Mater. Sci. Lett.* **1**, 145 (1982).  
<sup>28</sup>O. Bostanjoglo, *Phys. Status Solidi A* **76**, 525 (1983).  
<sup>29</sup>J. L. Brimhall, *J. Mater. Sci.* **19**, 1818 (1984).  
<sup>30</sup>H. J. Leamy, W. L. Brown, G. K. Celler, G. Foti, G. H. Gilmer, and J. C. C. Fan, *Appl. Phys. Lett.* **38**, 137 (1981).  
<sup>31</sup>R. B. Gold, J. F. Gibbons, T. J. Magee, J. Peng, R. Ormond, V. R. Deline, and C. A. Evans, Jr., in *Laser and Electron Beam Processing of Materials*, edited by C. W. White and P. S. Peercy (Academic, New York, 1980), pp. 221–226.  
<sup>32</sup>R. K. Sharma, S. K. Bansal, R. Nath, R. M. Mehra, Kanwar Bahadur, R. P. Mall, K. L. Chaudhary, and C. L. Garg, *J. Appl. Phys.* **55**, 387 (1984).  
<sup>33</sup>M. Oron and G. Sorensen, *Appl. Phys. Lett.* **35**, 782 (1979).  
<sup>34</sup>H. J. Leamy, G. A. Rozgonyi, and T. T. Sheng, *Appl. Phys. Lett.* **32**, 535 (1978).  
<sup>35</sup>G. N. Maracas, G. L. Harris, C. A. Lee, and R. A. McFarlane, *Appl. Phys. Lett.* **33**, 453 (1978).

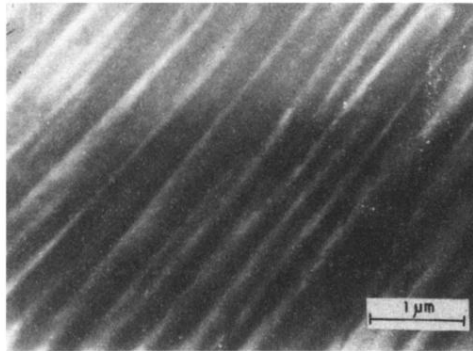


(a)

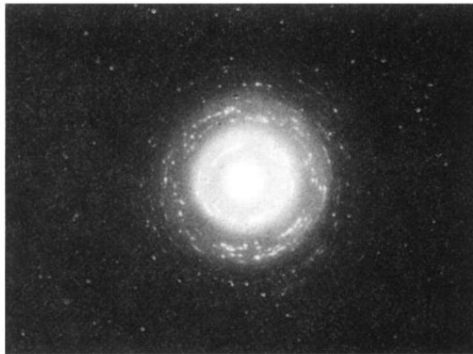


(b)

**FIG. 1.** (a) Electron micrograph of initial  $\text{Se}_{80}\text{Te}_{20}$  film ( $\times 10\,000$ ). (b) Selected area diffraction pattern of the region in (a) showing amorphous nature of the initial film.

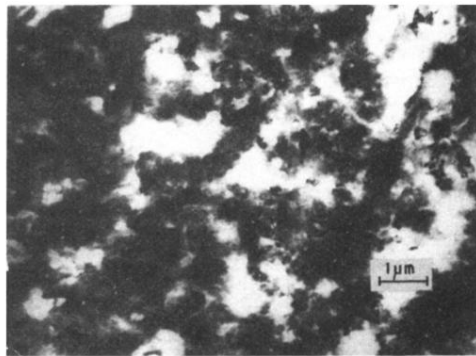


(a)

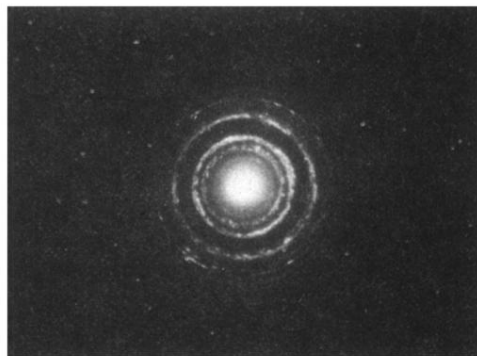


(b)

**FIG. 2.** (a) Same region as of Fig. 1(a) after some electron bombardment ( $\times 20\,000$ ). (b) Selected area diffraction pattern of the region in (a).

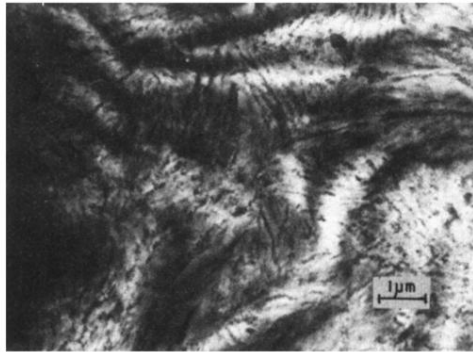


(a)

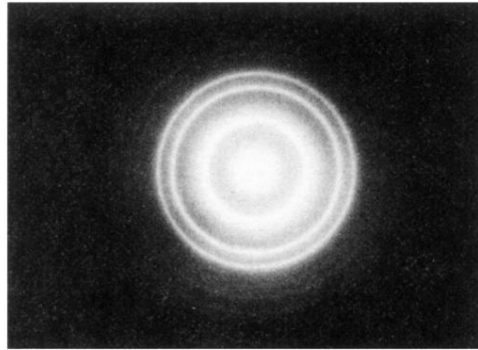


(b)

**FIG. 3.** (a) Same region as of Figs. 1(a) and 2(a) after further bombardment ( $\times 10\,000$ ). (b) Selected area diffraction pattern of the region in (a).



(a)



(b)

FIG. 4. (a) Electron micrograph showing the effect of increased beam intensity ( $\times 10\,000$ ). (b) Selected area diffraction pattern of the region in (a).

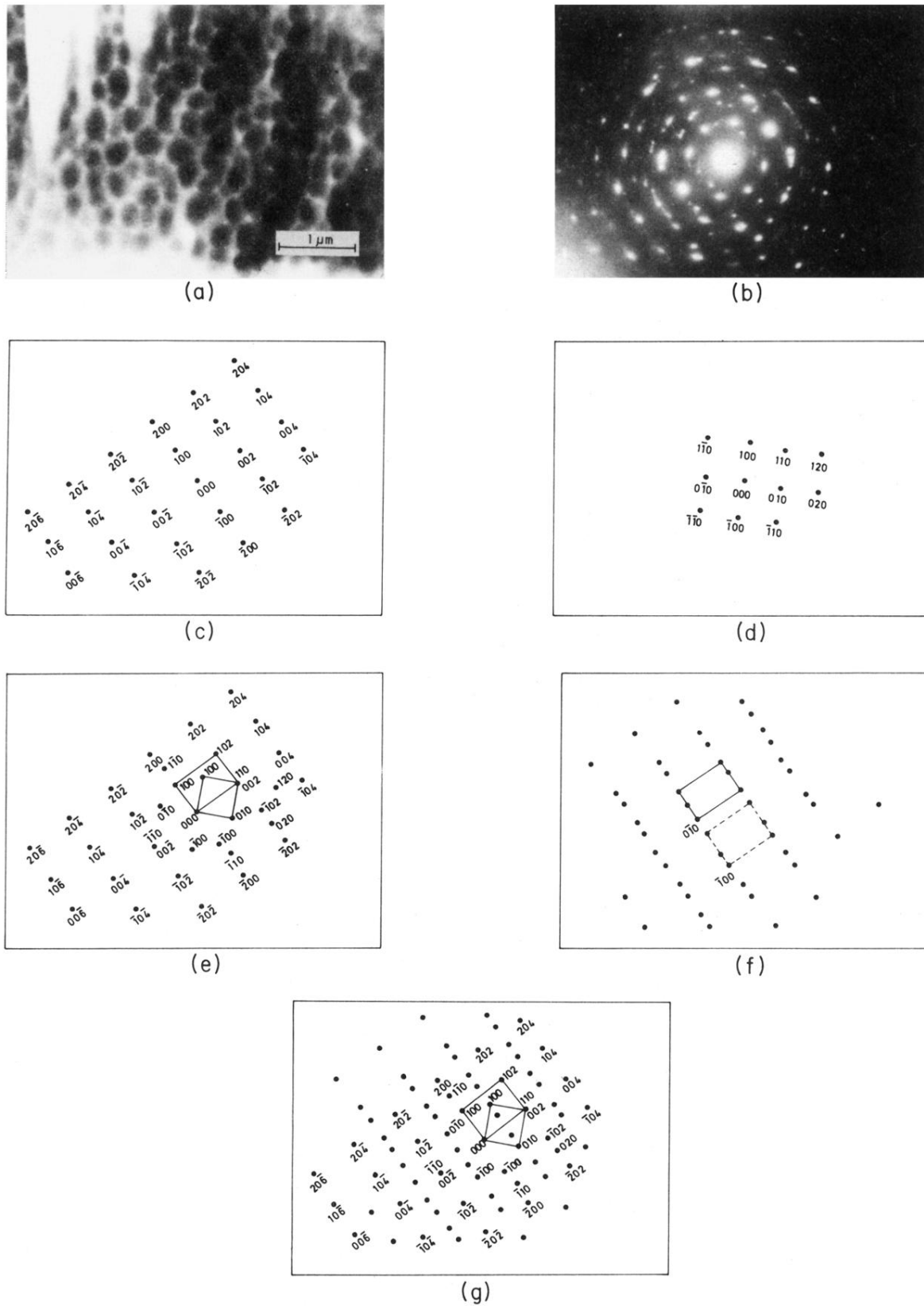


FIG. 5. (a) Electron micrograph of another amorphous specimen after bombardment showing single-crystalline aggregates with apparently hexagonal morphology ( $\times 20\,000$ ). (b) Selected area diffraction pattern of the region in (a). (c) (010) reciprocal-lattice section of  $\text{Se}_{80}\text{Te}_{20}$ . (d) (001) reciprocal-lattice section of  $\text{Se}_{80}\text{Te}_{20}$ . (e) Composite reciprocal-lattice point network (CRLP network) formed by superposing the two lattice sections in (c) and (d). (f) Reciprocal-lattice point networks corresponding to (010) reciprocal-lattice section with origins at  $010$  and  $100$  reciprocal-lattice points of (001) reciprocal-lattice section. (g) CRLP network formed by superposing the reciprocal-lattice point networks of (e) and (f).